Directly Dating Molybdenum-Copper Porphyry and Zinc-Silver-Lead-Copper-Gold Carbonate Replacement Deposit Mineralization in Northwestern British Columbia (NTS 104M/1)

S. Bowie[1], School of the Environment and Life Sciences, University of Portsmouth, Portsmouth, United Kingdom, sarah.bowie@port.ac.uk

C. Mottram, School of the Environment and Life Sciences, University of Portsmouth, Portsmouth, United Kingdom

D. Kellett, Geological Survey of Canada–Atlantic, Dartmouth, Nova Scotia

M. Barrington, Core Assets Corp., Atlin, British Columbia

C. Pike, Core Assets Corp., Nelson, British Columbia

Bowie, S., Mottram, C., Kellett, D., Barrington, M. and Pike, C. (2025): Directly dating molybdenum-copper porphyry and zinc-silver-lead-copper-gold carbonate replacement deposit mineralization in northwestern British Columbia (NTS 104M/1); *in* Geoscience BC Summary of Activities 2024, Geoscience BC, Report 2025-01, p. 15–26.

Introduction

Understanding tectonic controls on mineralization is central to locating and modelling ore deposits and reducing the socio-environmental footprint of exploration efforts. During collisional mountain-building events, faults and shear zones are known to act as planes of weakness, facilitating the migration of magma and associated mineralizing fluids up through the crust (e.g., Arndt, 2005; Sillitoe, 2010). Evidence of this fluid flow can be preserved in the form of mineralized quartz-carbonate veins that are localized or controlled by fault zones. Methods appropriate for dating magmatic and high-temperature ore-forming processes (such as U-Pb zircon and Re-Os molybdenite dating) cannot quantify important hydrothermal processes that may (re)deposit metals in many systems in the mid- to upper crust. However, recent developments in in-situ U-Pb carbonate geochronology now allow for these lower temperature fluid-flow and mineralization processes to be directly dated (e.g., Rasbury and Cole, 2009; Roberts et al., 2020; Mottram et al., 2024), providing important timing controls for petrogenetic models.

This project aims to directly date fluid flow, faulting and mineralization in a porphyry-epithermal-carbonate replacement deposit (CRD) to understand the timing, rates and duration of fluid flow and metal (re)distribution. It focuses on a new discovery in northwestern British Columbia (BC) associated with the Llewellyn fault, which structurally controls many epithermal and porphyry Cu-Au deposits in the Atlin Mining District north of the Golden Triangle (Figure 1a; e.g., Hart and Pelletier, 1989; Love et al., 1998; Mihalynuk et al., 2003; Ootes et al., 2017, 2018; Millonig et al., 2017). The Blue property, owned and operated by Core Assets Corp., hosts several mineralization styles: Mo-Cu porphyry, Zn-Cu-Ag skarn and Ag-Zn-Pb-Cu CRD in several target areas (e.g., Sulphide City, Jackie; Figure 1). Mineralized zones display evidence of multiple complex magmatic faulting and fluid-flow events that currently have no quantitative geochronological constraints. Therefore, the case-study system is ideal for applying U-Pb carbonate dating methodology to link the timing(s), rate and duration of mineralizing events to the tectonic and metallogenic framework of northwestern BC. Where possible, carbonate dates will be combined with higher temperature geochronometers (e.g., U-Th-Pb zircon, monazite, garnet, apatite and titanite, and/or Re-Os molybdenite), and trace-element data, to track the evolution of mineralization from the magmatic to hydrothermal regime (~800 ºC to ~200 ºC).

Geological Setting

The western margin of North America has undergone >200 million years of accretionary orogenesis, processes that continue to be active today (e.g., Coney, 1980; Colpron et al., 2007; Monger and Gibson, 2019). This long-lived tectonic history has resulted in a patchwork of commonly fault-bounded crustal fragments that make up the terranes of the Canadian-Alaskan Cordillera (Coney, 1980; Nelson and Colpron, 2007). These terranes can be grouped into five distinct morphogeological belts (Figure 1a; e.g., Nelson and Colpron, 2007; Soucy La Roche et al., 2022). Of these, the Intermontane Belt extends from south-central BC to central Yukon and comprises allochthonous pericratonic terranes associated with subduction-related arcs (Yukon-

---

[1] The lead author is a 2024 Geoscience BC Scholarship recipient.

This publication is also available, free of charge, as colour digital files in Adobe Acrobat® PDF format from the Geoscience BC website: https://geosciencebc.com/updates/summary-of-activities/.

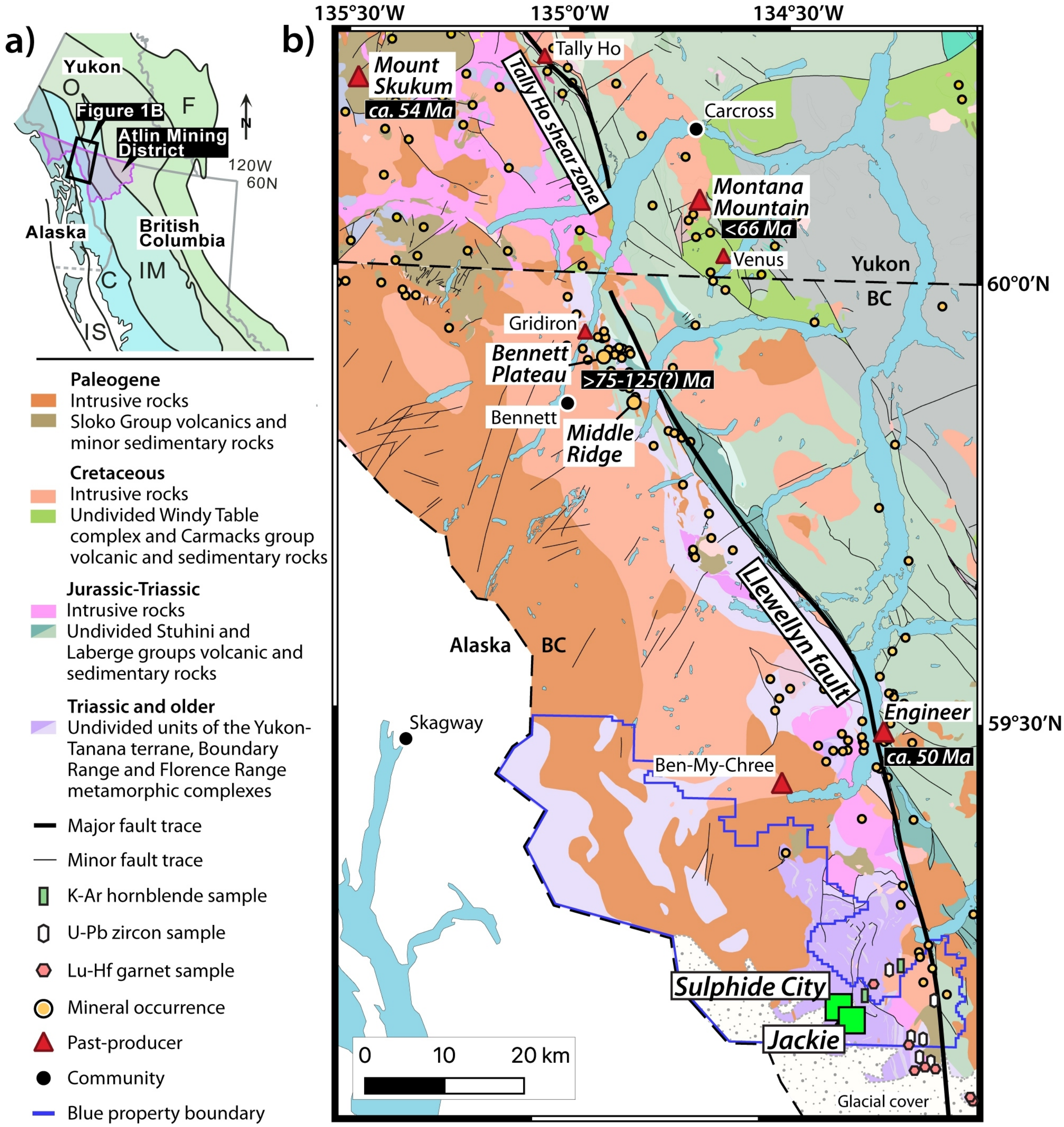

Figure 1. **a)** Morphogeological belts of the Canadian-Alaskan Cordillera (modified from Gabrielse et al., 1991). Atlin Mining District boundaries shown in purple, and area shown in Figure 1b is indicated by black box. Abbreviations: IS, Insular; IM, Intermontane; C, Coast; O, Omineca; F, Foreland. **b)** Simplified geology of southwestern Yukon and northwestern British Columbia, showing locations of mineral occurrences and past-producing mines. Cache Creek terrane units are undifferentiated and shown in grey. Sulphide City and Jackie sites within the Blue property are shown with green squares. Geology after Doherty and Hart (1988), Hart and Pelletier (1989), Hart and Radloff (1990), Mihalynuk (1999) and Ootes et al. (2018), and includes data from MapPlace (BC Geological Survey, 2006) and Yukon MINFILE (Yukon Geological Survey, 2020),. U-Pb zircon, K-Ar hornblende and Lu-Hf garnet sample locations from, Currie and Parrish (1997), Armstrong (unpublished data, BC Geological Survey, 2006) and Dyer (2020); see text for ages. Estimated ages of mineralization shown in black are from Hart and Pelletier (1989; Montana Mountain), Love et al. (1998), Mihalynuk et al. (2003; Middle Ridge), Millonig et al. (2017; Engineer and Mount Skukum) and Ootes et al. (2018; Bennett Plateau). Base map information from Yukon map data (https://map-data.service.yukon.ca/geoyukon/Administrative_Boundaries/Territorial_Provincial_Borders_1M).

Tanana, Stikinia, Quesnellia), and accretionary complexes made up of oceanic-floor sedimentary and volcanic rocks (Cache Creek, Slide Mountain; e.g., Colpron and Nelson, 2011; Monger and Gibson, 2019).

In northwestern BC, rocks that constitute Stikinia include the upper Triassic to middle Jurassic volcano-sedimentary Stuhini and Laberge Groups, as well as associated plutonic suites (Mihalynuk, 1999, Figure 1b). Within the Yukon-Tanana terrane, units include pervasively deformed greenschist to upper-amphibolite grade Proterozoic to early Paleozoic continental margin strata (Mihalynuk, 1999). Stratigraphic units include the Florence Range metamorphic suite of quartz-rich metapelitic rocks, marble, quartzite and amphibolite (Figure 1b; e.g., Jackson et al., 1991). This suite has been correlated with the pre-Late Devonian Snowcap assemblage in Yukon (Mihalynuk, 1999; Piercey and Colpron, 2009) and may have undergone several tectonometamorphic events between ca. 270 Ma and ca. 120 Ma (Currie, 1994; Dyer, 2020; Soucy La Roche et al., 2022). Also present in this region is the Boundary Range metamorphic suite, which consists of marble and limestone as well as chlorite-actinolite and quartzofeldspathic schists (Soucy La Roche et al., 2022). At present, the age and provenance of this unit remain unclear, although metamorphism likely postdates the emplacement of an Early Mississippian pluton (Currie and Parrish, 1997; Soucy La Roche et al., 2022) and Lu-Hf ages indicate garnet growth occurring from ca. 202 to 192 Ma (Dyer, 2020).

Llewellyn Fault System

The Llewellyn fault is a steeply dipping, northwest-striking brittle fault network that stretches ~180 km from northwestern BC to southwestern Yukon, where it may overprint the ductile Tally Ho shear zone (Ootes et al., 2017, 2018). In the Atlin Mining District, this fault may lie along a major terrane boundary between the Yukon-Tanana terrane to the west and the Stikine terrane to the east (Figure 1b; e.g., Hart and Radloff, 1990; Mihalynuk, 1999). Few previous studies have directly dated this fault; however, it is thought to have both ductile (ca. 120–75 Ma) and brittle deformation phases (ca. 56–50 Ma; Hart and Radloff, 1990; Ootes et al., 2017, 2018). Along strike, rocks are penetratively deformed, with south-southeast-trending foliations, lineations and folds that may indicate an overall sinistral sense of shear (Mihalynuk, 1999; Ootes et al., 2018). It is suggested that ductile deformation associated with the Llewellyn and Tally Ho deformational corridor postdates deposition of the Jurassic Laberge Group (Kellett and Zagorevski, 2022); and, while parallel deformational fabrics may be present in Triassic and older units, it remains difficult to definitively link them to a specific fault zone (Mihalynuk, 1999; Ootes et al., 2018). Along the Llewellyn fault zone, brittle deformation has been constrained to ca. 56–50 Ma north of the study site using U-Pb zircon ages from crosscutting plutons and ^{40}Ar-^{39}Ar vein adularia and vanadian illite ages from the Engineer and Mount Skukum mines (Love et al., 1998; Millonig et al., 2017; Ootes et al., 2018). This deformation overprints earlier ductile deformation fabrics that are likely analogous to the Tally-Ho shear zone (Figure 1b; Ootes et al., 2018).

The Llewellyn fault is spatially associated with more than 50 mineral occurrences in this region (Figure 1b), including epithermal, mesothermal and intrusion-related Au (Hart and Pelletier, 1989; Mihalynuk, 1999, Mihalynuk et al., 2003; Millonig et al., 2017; Ootes et al., 2017, 2018). At the Engineer and Mount Skukum mines (Figure 1b), it is thought that epithermal Au mineralization may be related to Eocene faulting following pluton emplacement (Love et al., 1998; Castonguay et al., 2017; Millonig et al., 2017; Ootes et al., 2017). However, more recent evidence also suggests that at least some intrusion-related Au mineralization at Middle Ridge and Bennett Plateau likely underwent ductile deformation and therefore predates the brittle Eocene phase of faulting in this region (Ootes et al., 2018).

Case-Study Ore Deposit

The Blue property (Core Assets Corp.), located ~50 km southwest of Atlin, BC and ~20–60 km east-southeast of Skagway, Alaska, is spatially proximal to the Llewellyn deformation corridor and comprises Jurassic, Cretaceous and Eocene intrusive units of the Boundary and Florence Range metamorphic suites (Figures 1b, 2; Currie and Parrish, 1993). Recent work focused on the Wann River shear zone near the base of the Willison glacier has shown that ductile deformation within the pre-Late Devonian Florence Range suite may be related to two regional metamorphic events, ca. 270–240 Ma and ca. 195–170 Ma, followed by localized contact metamorphism after ca. 120 Ma (Soucy La Roche et al., 2022). Similarly, Lu-Hf ages from the same area indicate that garnet growth occurred at ca. 190 Ma and ca. 185 Ma (Dyer, 2020). Proximal to the Llewellyn fault, what are interpreted to be zircon crystallization ages of ca. 103 to ca. 101 Ma were obtained from a large plutonic unit, and ages of ca. 352, ca. 335, ca. 191 and ca. 189 Ma were obtained from small granitic dikes near the Llewellyn glacier (Figure 2b; Currie and Parrish, 1997). Near the Willison glacier, previous studies obtained hornblende and biotite K-Ar cooling ages of ca. 144 Ma and ca. 97–96 Ma from amphibolite and granodiorite units, respectively (Armstrong and Werner, unpublished data, BC Geological Survey, 2006). At present there are few absolute geochronological constraints on brittle faulting, mineralized igneous units or fluid-flow processes in the region. This study aims to quantify the thermal-fluid–mineralization evolution of this case-study deposit system and test whether mineralization at the Blue property is temporally related to 1) major regional intrusive units; 2) deformation along the

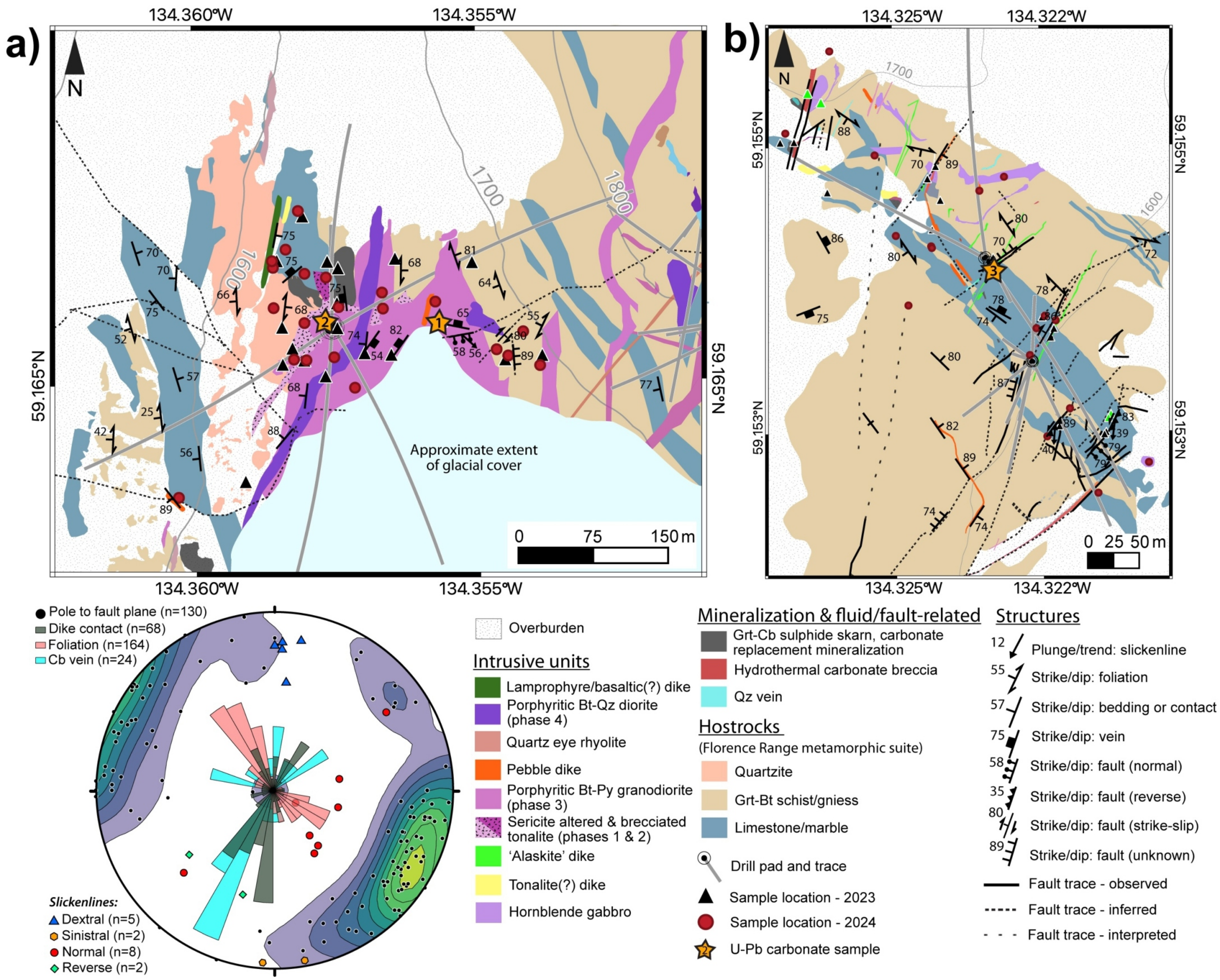

Figure 2. Schematic deposit-scale maps of the Sulphide City (**a**) and Jackie (**b**) showings within the Blue property (Core Assets Corp.). Locations of samples with U-Pb carbonate dates included in this paper are shown with numbered orange stars: 1) 23SB-013B1; 2) SLM22-006-396.0; and 3) SLM22-002-95.53. Stereonet displays field data from both showings and includes Rose diagrams showing the trends of dike contacts, gneissic foliation and carbonate veins. Slickenlines are plotted by dominant shear sense (dextral, sinistral, normal or reverse). Poles to fault planes are contoured at 1 intervals. Maps modified, with permission, from a Core Assets Corp. assessment report (Rodway and Barrington, 2024) and plotted with EPSG:4326–WGS 84 datum. Abbreviations: Bt, biotite; Cb, carbonate; Grt, garnet; Pb, lead; Py, pyrite; Qz, quartz; U, uranium.

Llewellyn fault or other smaller fault splays; and/or 3) several overprinting mineralizing magmatic-hydrothermal events.

Field Observations and Relationships

Fieldwork carried out in July 2023 and July 2024 focused on the 'Sulphide City' and 'Jackie' showings (Figures 1b, 2) within the Blue property. Hostrocks comprise southeast-striking, steeply dipping and polyphase folded marble and garnet-biotite gneiss of the Florence Range metamorphic suite (Figures 1b, 2; e.g., Mihalynuk, 1999). Mineralization styles range from Mo-Cu porphyry and Fe-Zn-Cu skarn at Sulphide City to Zn-Ag-Pb-Cu-Au CRD, massive to semimassive sulphide skarn and distal epithermal veins at Jackie. Mineralized zones correlate with proximity to surficial exposures of ~5–200 m wide porphyritic tonalitic to granodioritic intrusions and ~15–50 cm wide mafic to intermediate dikes. Northeast-striking, steeply dipping brittle faults commonly crosscut the dominantly northwest-trending lithological contacts between gneiss and marble units, as well as younger dikes and plutonic units (Figure 2), and may also correlate with areas of increased mineralization and fluid alteration. Fault planes variably contain ~1-2 cm thick quartz, carbonate and, more rarely, zinc- and/or iron-oxide infill.

Sulphide City

Intrusive units, ~5–200 m wide, are observed at Sulphide City and include mineralized tonalitic to granodioritic rocks that can be divided into four phases based on field relationships. Exposed at the edges of the central intrusive body (phase 3; Figures 2a and 3), phases 1 and 2 may be defined as diatreme/magmatic-hydrothermal breccias and are challenging to differentiate. Due to pervasive sericite alteration, the clasts, ranging from <1 cm to 10 cm, are difficult to identify but may be composed primarily of felsic igneous material containing ~1–2 mm quartz eyes and biotite and feldspar porphyroclasts. In places, clasts of Zn-Fe-Cu massive sulphide associated with phase 1 occur within phase 2 (Figure 3b). The matrix contains quartz and sericite-altered feldspar <1 mm in size and, in places, disseminated pyrite and pyrrhotite mineralization ~2-5 mm in size.

Phase 3 is composed of light grey, massive granodiorite. It has a porphyritic texture, with 2–3 mm plagioclase and 1-2 mm biotite phenocrysts (~5%) in a fine crystalline matrix composed dominantly of quartz (~50%), plagioclase (~30-40%) and K-feldspar (~10-20%; Figure 3a). It also hosts ~0.1–0.5 cm crystals of porphyry-style pyrite, pyrrhotite and molybdenite mineralization, both in generally west-dipping ~0.2–0.5 cm wide stringers and disseminated throughout the matrix. Chalcopyrite mineralization is less common at the surface but may occur with pyrrhotite as ~0.1–0.5 cm crystals disseminated within the matrix and increasing in abundance with depth. This unit is not pervasively brecciated, but in places contains rare clasts of massive sulphide and garnet skarn mineralization. At the surface, phase 3 generally displays a lower degree of sericite alteration than phases 1 and 2, and plagioclase phenocrysts are less pervasively altered.

Phase 4 is a northwest-striking, steeply dipping, unmineralized diorite dike approximately ~5-6 m wide. It has a porphyritic texture containing ~1-2 mm biotite phenocrysts (~10-15%) and less quartz than phases 1 to 3 (~30–40%). It appears largely unaltered by sericite or skarn alteration, and phenocrysts of plagioclase and biotite appear euhedral and intact on fresh surfaces. Therefore, this unit likely postdates igneous mineralizing activity. It has a ~1 m wide chilled margin defined by a fining of crystal size from ~5-10 mm to <2 mm that visibly crosscuts phases 2 and 3 and contains rounded xenoliths similar in composition to phase 3.

Carbonate minerals are present at Sulphide City in an array of settings, including as ~0.5–3 cm wide deformed veins within the gneissic and marble country rocks; fault breccia infill and slickenfibres; crystals intergrown with pyrite, pyrrhotite, chalcopyrite, sphalerite, epidote and garnet; and as barren and undeformed veins crosscutting mineralized units (Figure 3c, d). Skarn mineralization at Sulphide City is observed at the margins of phases 1 to 3, occurring mainly at northwest-trending, steeply dipping contacts between marble and garnet-biotite gneiss hostrock units (Figure 3e), at contacts between hostrock units and predeformational felsic sills and dikes, and within north- to west-northwest-trending hinge zones in doubly plunging marble folds. Both exoskarn and endoskarn mineralization occurs across the showing. Exoskarn is observed as massive replacement of marble and as smaller ~10–50 cm pods along fracture surfaces (Figure 3d). Prograde assemblages include ~0.1–1 cm wollastonite needles, ~0.2–1 cm red to light brown zoned garnet and dark green augite in a very fine (<0.5 mm) crystalline sericite-quartz-carbonate matrix (Figure 3d, e); ~0.2–1 cm, light green- to brown-zoned vesuvianite may also be present in places. These areas are often spatially associated with retrograde assemblages of quartz, carbonate, epidote, chlorite and massive sulphide mineralization (Py+Ccp+Po+Sp±Gn; Figure 3e). Although also observed in phases 2 and 3, endoskarn alteration is especially well developed in phase 1 as massive garnet, augite, epidote and chlorite, along with rusty orange-weathering massive sulphide (Py+Po+Gn+Sp) mineralization. With increasing distance (e.g., >50 m) from intrusive phases 1–3, both prograde and retrograde skarn assemblages reduce in intensity.

Jackie

The Jackie showing comprises mainly southeast-striking marble and garnet-biotite gneiss country rocks with gener-

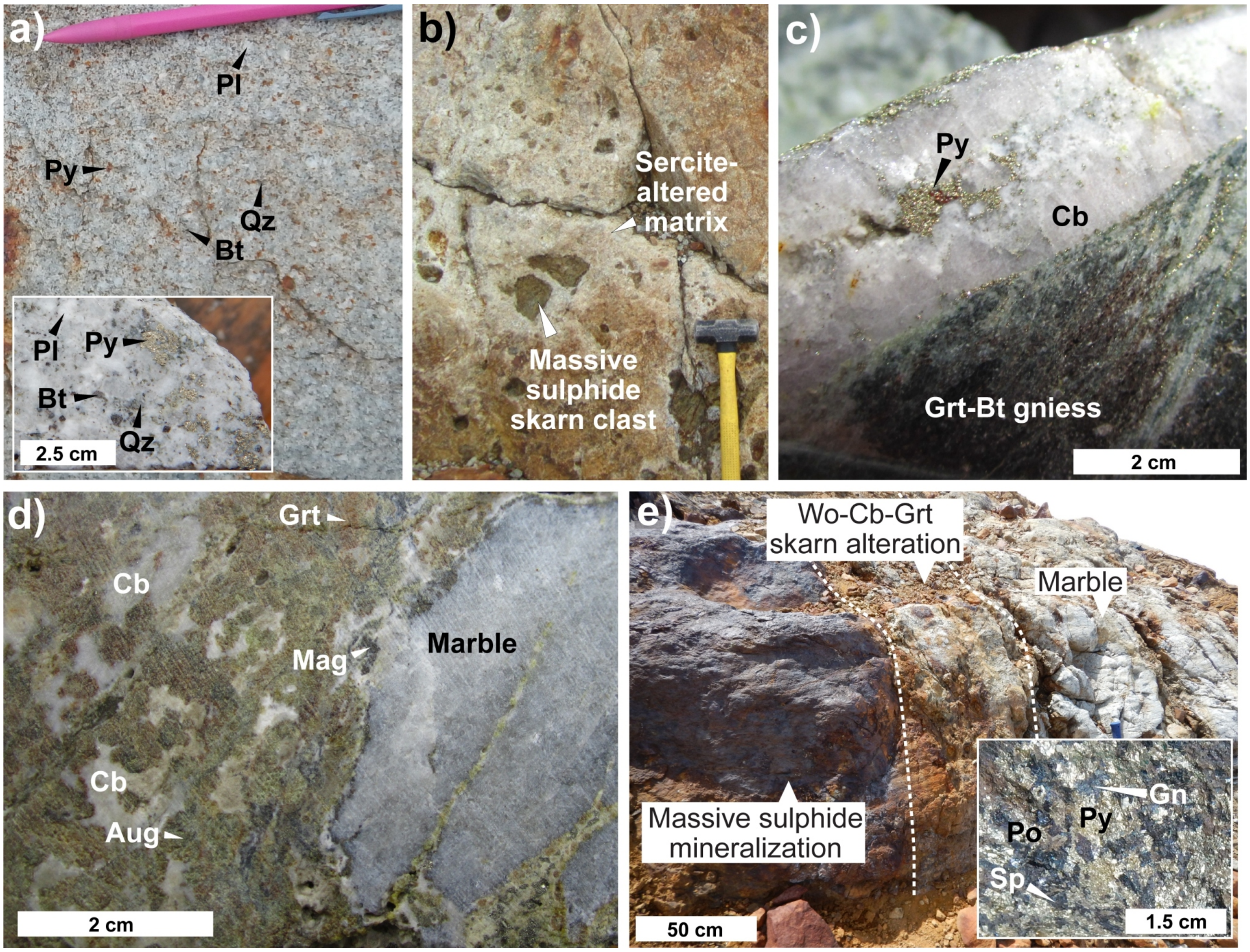

Figure 3. Examples of intrusive units and mineralization styles at Sulphide City: **a)** porphyry-style mineralization in granodiorite (phase 3) containing disseminated and vein-hosted pyrite, molybdenite and chalcopyrite; **b)** massive sulphide skarn clasts within the highly sericite-altered matrix of phase 2; **c)** pyrite mineralization within a carbonate vein crosscutting deformed and altered garnet-biotite gneiss hostrock; **d)** carbonate-garnet-augite-magnetite skarn mineralization partially replacing marble hostrock; **e)** rusty-weathering, massive sulphide mineralization and wollastonite-carbonate-garnet skarn alteration at the margin of marble hostrock. Inset shows detail of texture within the massive sulphide mineralization zone. Abbreviations: Aug, augite; Bt, biotite; Cb, carbonate; Grt, garnet; Gn, galena; Mag, magnetite; Pl, plagioclase; Po, pyrrhotite; Py, pyrite; Sp, sphalerite; Wo, wollastonite.

ally east-southeast-trending complex folds crosscut by several intrusive units (Figure 2b). Crosscutting intrusions include 1) ~2–3 m wide, northeast- to east-striking hornblende gabbro dikes that, in places, host pyrite mineralization in ~1 mm wide veins; 2) <1 m wide, typically northeast-striking, often aphanitic, light green–weathering intermediate 'alaskite' dikes (Figure 4a); 3) ~0.5–1 m wide north-northwest- to northwest-trending mineralized pebble dikes that crosscut host rocks and are composed of ~1–15 cm, rounded to subrounded clasts of marble and garnet-biotite gneiss, mineralized tonalite to granodiorite, and massive sulphide skarn mineralization (Figure 4b). Pebble dikes are largely clast supported and have matrices consisting of ~85–95% hydrothermal quartz and carbonate, and ~5–15% rock flour and sulphide minerals. Pyrrhotite-sphalerite-galena-chalcopyrite CRD mineralization commonly occurs in centimetre- to metre-scale amorphous pods and massive replacement zones, ~1-2 cm wide veins and at northwest-striking contacts between marble and the 'alaskite' dikes (Figure 4a, c).

Steeply dipping, northeast-trending brittle faults crosscut all lithologies present at Jackie, including mineralized units and typically show evidence for centimetre- to metre-scale offsets (Figure 4d). Carbonate, wollastonite and/or iron-oxide slickenfibres are commonly observed on fault surfaces and suggest a mixture of normal, reverse and strike-slip motion, with both sinistral and dextral displacement, across the showing (Figure 2b). Although the 'alaskite' dikes are often crosscut and offset by faults, faulting is also observed parallel to and at northwest-striking contacts be-

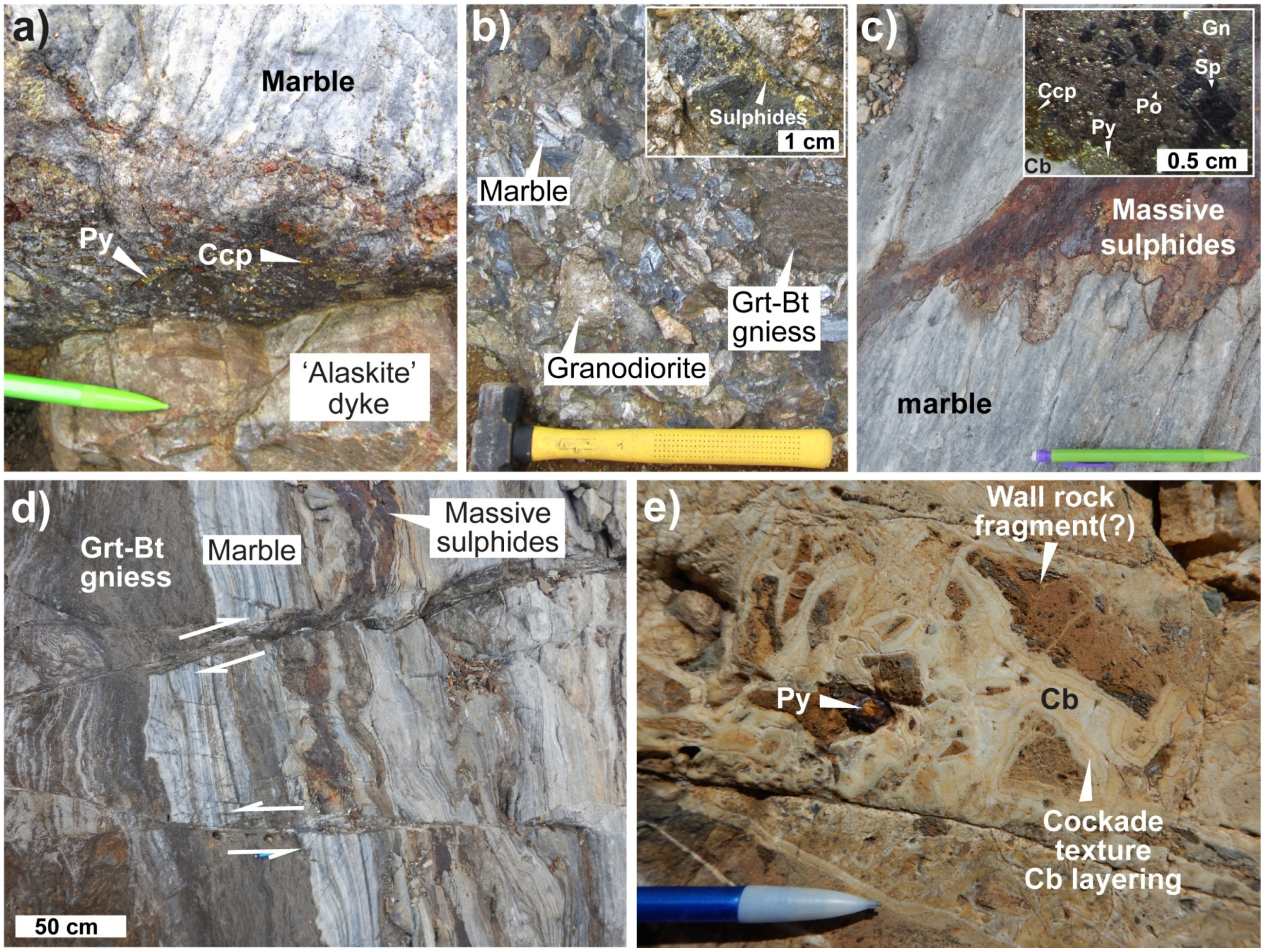

Figure 4. Mineralization at the Jackie showing: **a)** pyrite and chalcopyrite mineralization at the contact between an 'alaskite' dike and marble host rock; **b)** pebble dike containing marble, granodiorite and garnet-biotite gneiss clasts; inset shows clast containing sulphide mineralization; **c)** carbonate replacement-style sulphide mineralization in marble; massive sulphide texture detail shown in inset; **d)** ~50–75 cm offset on a conjugate fault set crosscutting mineralized bands within marble host rock; **e)** hydrothermal Fe-rich carbonate with cockade textures infilling a ~1–2 m wide fault zone and containing disseminated pyrite mineralization. Abbreviations: Bt, biotite; Cb, carbonate; Ccp, chalcopyrite; Gn, galena; Grt, garnet; Po, pyrrhotite; Py, pyrite; Sp, sphalerite.

tween the dikes and host rocks. At the NW margin of the showing, a north-northeast-striking fault contains a ~2–3 m wide zone of hydrothermal breccia comprising ~1–5 cm clasts surrounded by cockade texture Fe-rich carbonate and disseminated pyrite (Figure 4e).

Methodology

In situ U-Pb carbonate dating via laser ablation–inductively coupled plasma–mass spectrometry (LA-ICP-MS) was carried out at the University of Portsmouth to determine the temporal evolution of fluid flow within the two study areas described above (methodology follows that described in Parrish et al. (2018) and Mottram et al. (2024)).

Table 1. Summary of sample locations for U-Pb dating and preliminary age information.

Showing	Field sample	Drillhole no.	Sample depth (m)	Drillhole dip	Latitude	Longitude	Mineral analyzed	n	Date (Ma)[1]	MSWD	Average U (ppm)[2]
Sulphide City	23SB-013B1	n/a	Surface	n/a	59.165569	-134.355588	Carbonate	57	56.2 ±2.5	2.0	1.4
Sulphide City	n/a	SLM22-006	396.0	50°	59.165556	-134.357505	Carbonate	45	54.0 ±6.5	1.5	0.2
Jackie	n/a	SLM22-002	95.53	90°	59.153966	-134.323381	Carbonate	33	51.0 ±4.8	1.3	0.3

[1] Quoted uncertainties are 2σ and include propagated uncertainty

[2] Semiquantitative estimate

Abbreviation: MSWD, mean square weighted deviation

Latitude and longitude co-ordinates use EPSG:4326–WGS 84 datum

Samples were first characterized via optical and reflected light, scanning electron microscopy (SEM) and electron dispersive spectroscopy (EDS). Carbonate minerals were targeted from a range of pre-, syn- and post-mineralization vein and fault settings (Figures 3, 4, 5). Quoted uncertainties in Table 1 and Figure 5 are 2σ and include 2% additional propagated uncertainty to account for the dispersion and long-term reproducibility of the secondary reference materials: Duffbrown limestone (64 ±2 Ma; Hill et al., 2016) and Mudtank zircon (732 ±5 Ma; Black and Gulson, 1978; Jackson et al., 2004). Where applicable, in situ U-Pb skarn garnet dating and any targeted accessory minerals will follow a similar methodology (e.g., Seman et al., 2017).

Preliminary Geochronology Results

Preliminary U-Pb carbonate dates from samples collected at the Sulphide City and Jackie showings are presented in Table 1 and Figure 5. At Sulphide City, an ~1 cm wide blocky carbonate vein crosscutting mineralized granodiorite (phase 3) yielded an age of 56.2 ±2.5 Ma (n = 57; MSWD = 1.3). Similarly, an ~0.5 cm wide quartz-carbonate vein crosscutting large centimetre-scale pyrite cubes at Sulphide City yielded an age of 54.0 ±6.5 Ma (n = 45; MSWD = 1.5). At Jackie, ~0.2 cm wide pull-apart veins infilled with fine crystalline carbonate crosscut the foliation in garnet-biotite schist and yielded an age of 51.0 ±4.8 Ma (n = 33; MSWD = 2.0). Approximately 30 additional carbonate samples, representing a wide range of textures within the Sulphide City and Jackie showings, are currently being analyzed, as well as skarn garnets and igneous zircon in intrusive units.

First-Order Interpretations

Combined with field and drillcore observations, the preliminary dates obtained here provide the first temporal constraints on the timing of magmatic-hydrothermal fluid activity at the Sulphide City and Jackie showings. Carbonate ages date the timing of faulting, extensional crack-seal vein formation and fluid flow (e.g., Roberts et al., 2020; Mottram et al., 2020, 2024).

The preliminary ages obtained here broadly correlate with ages for epithermal gold mineralization at the Mount Skukum mine at ca. 54 Ma (adularia ^{40}Ar-^{39}Ar age) and Engineer mine at ca. 50 Ma (vanadian illite ^{40}Ar-^{39}Ar age), and

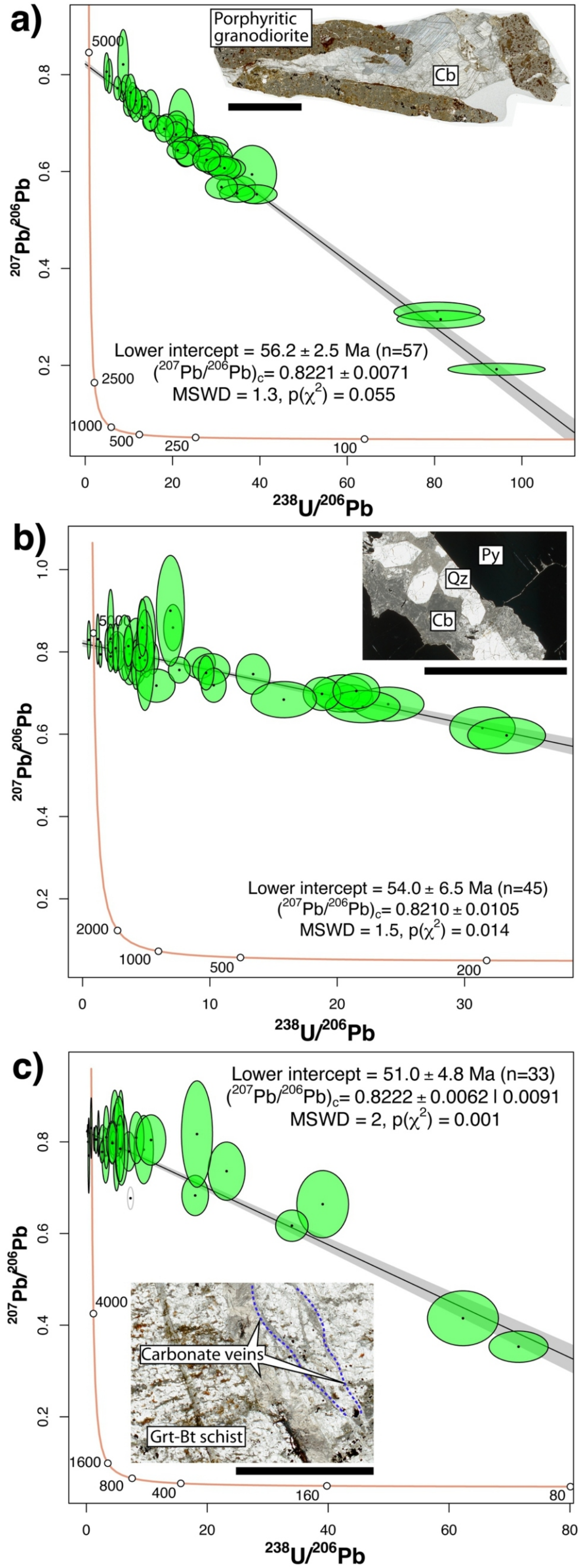

Figure 5. Preliminary U-Pb dates from carbonate samples (see Table 1 for details and Figure 2 for map locations): **a)** U-Pb date from a coarse crystalline carbonate (CB) vein crosscutting mineralized granodiorite at Sulphide City (sample SLM22-002-95.53); **b)** U-Pb date from quartz (Qz)-carbonate vein crosscutting ~3 cm pyrite (Py) crystals at Sulphide City (sample SLM22-006-396.0); **c)** U-Pb date from small pull-apart veins crosscutting marble host rock at Jackie (sample 23SB-013B1). All quoted uncertainties are 2ó and include propagated uncertainty. Black scale bars in all insets are 1 cm.

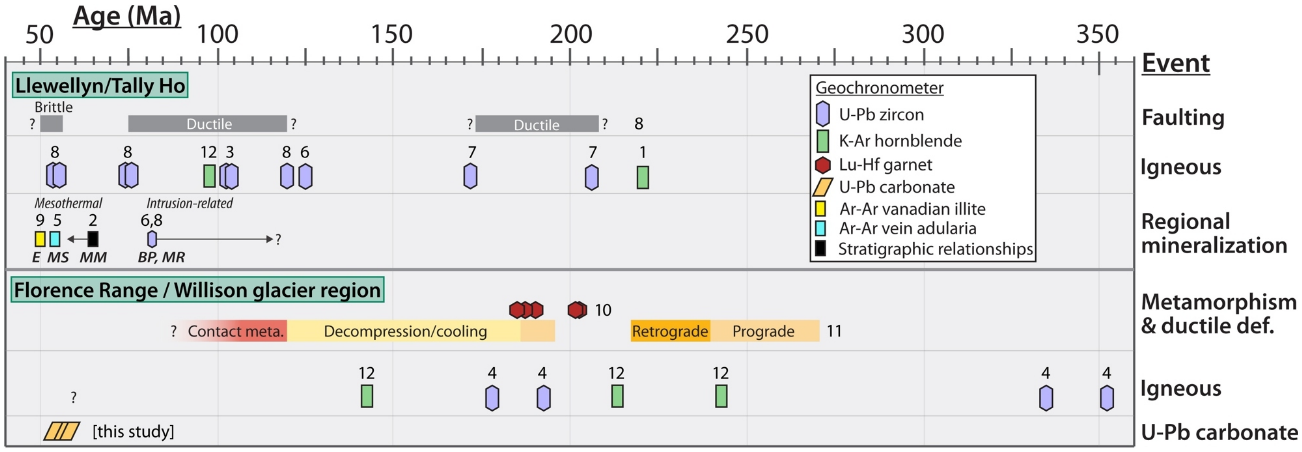

Figure 6: Compilation of current geochronological constraints on the Llewellyn fault–Tally Ho shear zone, deformation and metamorphism, and mineralization, northwestern British Columbia and southwestern Yukon. Dates included are from this study and [1] Bultman (1979), [2] Hart and Pelletier (1989), [3] Currie (1994), [4] Currie and Parrish (1997), [5] Love et al. (1998), [6] Mihalynuk et al. (2003), [7] Tizzard et al. (2009), [8] Ootes et al. (2018), [9] Millonig et al. (2017), [10] Dyer (2020), [11] Soucy La Roche et al. (2022) and [12] Armstrong and Werner (unpub. data, BC Geological Survey, 2006). See Figure 1b for spatial distribution of age constraints. Abbreviations: BP, Bennett Plateau; E, Engineer mine; MM, Montana Mountain; MR, Middle Ridge; MS, Mount Skukum mine.

mesothermal gold mineralization at Montana Mountain occurring after ca. 66 Ma, based on volcano-stratigraphic relationships (Figures 1, 6; Hart and Pelletier, 1989; Love et al., 1998; Millonig et al., 2017). Combined with existing regional ages, results indicate the widespread and protracted relationship between brittle deformation occurring along the Llewellyn fault, the intrusion of several overprinting phases of porphyritic granodioritic-tonalitic units, and a wide variety of mineralization styles.

Future Work

The next phase of this project will focus on combining several additional geochronometers, including zircon, garnet, titanite and apatite, spanning from igneous to hydrothermal temperatures, to thoroughly document the temporal evolution of the complex and interrelated igneous and mineralizing processes at the Blue property. U-Pb zircon dating of the major igneous phases, including the mineralized tonalite and granodiorite, will provide absolute constraints for the timing of igneous activity. The next steps for this project will therefore include analysis of additional carbonate and garnet samples, and the improvement of precision, where possible, for existing ages by carrying out more analyses to locate relatively high-U domains. Ongoing SEM and EDS imaging will be used to better characterize microstructures and minor mineral phases present in key samples. This imaging will also aid in identifying the textural context of additional accessory minerals that may be dated, including titanite, apatite and/or molybdenite. In addition, trace element analysis of dated carbonate and garnet crystals will aid in linking these minerals to mineralization processes, and provide context for differentiating fluid flow events. Comparing the age of intrusive units, skarn garnet growth, and carbonate vein and breccia crystallization will be critical for temporally constraining the rate and duration of both porphyry and skarn mineralization, as well as faulting events at the study sites.

Acknowledgments

The authors thank M. Shtereva, D. Šilerová, R. Martin, and L. Nania for their assistance in the field in 2023 and 2024, and G. Long, J. Dunlop and G. Chapman for laboratory support at the University of Portsmouth. S. Porter, L. Piccott, N. Rodway, S. Coutts, K. Smallwood and the rest of the Core Assets team are thanked for their help, both in the core library and at field sites. Thanks also to J. Luck and J. Cleveland of Interior Helicopters Ltd. for their expert helicopter support, and M. Mihalynuk for helpful discussion in the field. The authors gratefully acknowledge funding for this project provided by the University of Portsmouth and Core Assets Corp. (to S.B. and C.M.), the GEM-GeoNorth program of the Geological Survey of Canada (to D.K.), and NSERC PGS-D, Geoscience BC and SEG PhD scholarship programs (to S.B.). J. Darling and J. Cutts are thanked for their constructive reviews of this manuscript.

References

Arndt, N.T. (2005): The conduits of magmatic ore deposits; Chapter 9 *in* Exploration for Platinum-Group Element Deposits, J.E. Mungall (ed.), Mineralogical Association of Canada, v. 35, p. 181–201, URL <https://pubs.geoscienceworld.org/mac/books/edited-volume/2491/chapter/142153269/CHAPTER-9-THE-CONDUITS-OF-MAGMATIC-ORE-DEPOSITS> [October 2024].

BC Geological Survey (2006): MapPlace 2 GIS internet mapping system; British Columbia Ministry of Energy, Mines and Low Carbon Innovation, MapPlace website, URL <https://

www2.gov.bc.ca/gov/content/industry/mineral-exploration-mining/british-columbia-geological-survey/mapplace> [May 2023].

Black, L. and Gulson, B. (1978): The age of the Mud Tank carbonatite, Strangways Range, Northern Territory; Journal of Australian Geology and Geophysics, v. 3, p. 227–232.

Bultman, T.R. (1979): Geology and tectonic history of the Whitehorse trough west of Atlin, British Columbia; Ph.D. thesis, Yale University, 284 p.

Castonguay, S., Ootes, L., Mercier-Langevin, P., Rowins, S. and Devine, F. (2017): Orogenic gold along Cordilleran faults: key characteristics and analogies between Phanerozoic and Archean settings; Geological Survey of Canada, Open File 8199, p. 35–37, URL <https://doi.org/10.4095/299573>.

Colpron, M. and Nelson, J.L. (2011): A Digital Atlas of Terranes for the Northern Cordillera; British Columbia Ministry of Energy, Mines, and Low Carbon Innovation, BC Geological Survey, GeoFile 2011-11., 3 p. and 4 maps.

Colpron, M., Nelson, J.L. and Murphy, D.C. (2007): Northern Cordilleran terranes and their interactions through time; GSA Today, v. 17, no. 4/5, p. 4-10, URL <https://data.geology.gov.yk.ca/Reference/81668#InfoTab> [June 2024].

Coney, P.J. (1980): Cordilleran metamorphic core complexes: an overview; *in* Cordilleran Metamorphic Core Complexes, M.D. Crittenden Jr., P.J. Coney and G.H. Davis (ed.), Geological Society of America Memoirs, v. 153, p. 7–31, URL <doi:10.1130/MEM153-p7>.

Currie, L.D. (1994): The Geology and Mid-Jurassic amalgamation of Tracy Arm Terrane and Stikinia of northwestern British Columbia; Ph.D. thesis, Carleton University, 416 p.

Currie, L.D. and Parrish, R.R. (1993): Jurassic accretion of Nisling terrane along the western margin of Stikinia, Coast Mountains, northwestern British Columbia; Geology, v. 21, no. 3, p. 235–238, URL <doi:10.1130/0091-7613(1993)021<0235:JAONTA>2.3.CO;2>.

Currie, L.D. and Parrish, R.R. (1997): Paleozoic and Mesozoic rocks of Stikinia exposed in northwestern British Columbia: implications for correlations in the northern Cordillera; GSA Bulletin, v. 109, no. 11, p. 1402–1420, URL <doi:10.1130/0016-7606(1997)109<1402:PAMROS>2.3.CO;2>.

Doherty, R.A. and Hart, C.J.R. (1988): Preliminary geology of Fenwick Creek (105D/3) and Alligator Lake (105D/6) map areas; Yukon Geological Survey, Open File 1988-2, 2 maps, 1:50 000 scale.

Dyer, S. (2020): The Early Jurassic metamorphic history of the Yukon-Tanana terrane of northwestern British Columbia: insights from a new inverse garnet fractionation modelling technique; M.Sc. thesis, Carleton University, 314 p.

Gabrielse, H., Monger, J., Wheeler, J.O. and Yorath, C.J. (1991): Morphogeological belts, tectonic assemblages, and terranes; Chapter 2 *in* Geology of the Cordilleran Orogen in Canada, H. Gabrielse and C.J. Yorath, (eds.), Geological Survey of Canada, Geology of Canada, no. 4, p. 15–28.

Hart, C.J.R. and Pelletier, K.S. (1989): Geology of Carcross (105D/2) and part of Robinson (105D/7) map areas; Yukon Geological Survey, Open File 1989-1, 84 p., URL <https://emrlibrary.gov.yk.ca/ygs/open_files/1989/1989_1.pdf> [September 2023].

Hart, C.J.R. and Radloff, J.K. (1990): Geology of Whitehorse, Alligator Lake, Fenwick Creek, Carcross and part of Robinson map areas (105D/11, 6, 3, 2 & 7); Yukon Geological Survey, Open File 1990-4(G).

Hill, C.A., Polyak, V.J., Asmerom, Y. and Provencio, P.P. (2016): Constraints on a Late Cretaceous uplift, denudation, and incision of the Grand Canyon region, southwestern Colorado Plateau, USA, from U-Pb dating of lacustrine limestone; Tectonics, v. 35, no. 4, p. 896–906, URL <https://doi.org/10.1002/2016TC004166>.

Jackson, J.L., Gehrels, G.E., Patchett, P.J. and Mihalynuk, M.G. (1991): Stratigraphic and isotopic link between the northern Stikine terrane and an ancient continental margin assemblage, Canadian Cordillera; Geology, v. 19, no. 12, p. 1177–1180, URL <https://doi.org/10.1130/0091-7613(1991)019<1177:SAILBT>2.3.CO;2>.

Jackson, S.E., Pearson, N.J., Griffin, W.L. and Belousova, E.A. (2004): The application of laser ablation-inductively coupled plasma–mass spectrometry to in situ U–Pb zircon geochronology; Chemical Geology, v. 211, no. 1-2, p. 47–69, URL <https://doi.org/10.1016/j.chemgeo.2004.06.017>.

Kellett, D.A. and Zagorevski, A. (2022): The Jurassic Laberge Group in the Whitehorse Trough of the Canadian Cordillera: using detrital mineral deochronology and thermochronology to investigate tectonic evolution; Geoscience Canada, v. 49, p. 7–28, URL <doi:10.12789/geocanj.2022.49.183>.

Love, D.A., Clark, A.H., Hodgson, C.J., Mortensen, J.K., Archibald, D.A. and Farrar, E. (1998): The timing of adularia-sericite-type mineralization and alunite-kaolinite-type alteration, Mount Skukum epithermal gold deposit, Yukon Territory, Canada: ^{40}Ar-^{39}Ar and U-Pb geochronology; Economic Geology, v. 93, no. 4., p. 437–462, URL <https://doi.org/10.2113/gsecongeo.93.4.437>.

Mihalynuk, M.G. (1999): Geology and mineral resources of the Tagish Lake area (NTS 104M/ 8, 9, 10E, 15 and 104N/12W), northwestern British Columbia; BC Ministry of Energy, Mines and Low Carbon Innovation, BC Geological Survey, Bulletin 105, 235 p.

Mihalynuk, M.G., Devine, F.A.M. and Friedman, R.M. (2003): Marksmen partnership: potential for shallow submarine VMS (Eskay-style) and intrusive-related gold mineralization, Tutshi Lake area; Ministry of Energy, Mines and Low Carbon Innovation, BC Geological Survey, Geofile 2003-09, 1 p.

Millonig, L.J., Beinlich, A., Raudsepp, M., Devine, F., Archibald, D.A., Linnen, R.L. and Groat, L.A. (2017): The Engineer Mine, British Columbia: an example of epithermal Au-Ag mineralization with mixed alkaline and subalkaline characteristics; Ore Geology Reviews, v. 83, p. 235–257, URL <https://doi.org/10.1016/j.oregeorev.2016.12.023>.

Monger, J.W.H. and Gibson, H.D. (2019): Mesozoic-Cenozoic deformation in the Canadian Cordillera: the record of a 'Continental Bulldozer'?; Tectonophysics, v. 757, p. 153–169, URL <https://doi.org/10.1016/j.tecto.2018.12.023>.

Mottram, C.M., Kellett, D.A., Barresi, T., Chapman, G.G. and Halle, J. (2024): Tracking the porphyry-epithermal mineralization transition using U-Pb carbonate dating; Geology, v. 52, no. 9, p. 723–728, URL <https://doi.org/10.1130/G52211.1>.

Mottram, C.M., Kellett, D.A., Barresi, T., Zwingmann, H., Friend, M., Todd, A. and Percival, J.B. (2020): Syncing fault rock clocks: direct comparison of U-Pb carbonate and K-Ar illite fault dating methods; Geology, v. 48, no. 12, p. 1179–1183, URL <https://doi.org/10.1130/G47778.1>.

Nelson, J. and Colpron, M. (2007): Tectonics and metallogeny of the British Columbia, Yukon and Alaskan Cordillera, 1.8 Ga to the present; *in* Mineral Deposits of Canada: A Synthesis of Major Deposit-Types, District Metallogeny, the Evolution of Geological Provinces, and Exploration Methods, W.D. Goodfellow (ed.), Geological Association of Canada, Mineral Deposits Division, Special Publication No. 5, p. 755–791, <https://cmscontent.nrs.gov.bc.ca/geoscience/PublicationCatalogue/External/EXT060.pdf > [November 2024].

Ootes, L., Castonguay, S., Friedman, R., Devine, F. and Simmonds, R. (2018): Testing the relationship between the Llewellyn fault, Tally-Ho shear zone, and gold mineralization in northwest British Columbia; *in* Geological Fieldwork 2017, British Columbia Ministry of Energy, Mines and Low Carbon Innovation, British Columbia Geological Survey, Paper 2018-01, p. 67–81.

Ootes, L., Elliott, J.M., and Rowins, S.M. (2017): Testing the relationship between the Llewellyn fault, gold mineralization, and Eocene volcanism in northwest British Columbia: a preliminary report.; *in* Geological Fieldwork 2016, British Columbia Ministry of Energy, Mines and Low Carbon Innovation, British Columbia Geological Survey, Paper 2017-01, p. 49–59.

Parrish, R.R., Parrish, C.M. and Lasalle, S. (2018): Vein calcite dating reveals Pyrenean orogen as cause of Paleogene deformation in southern England; Journal of the Geological Society, v. 175, p. 425–442, URL <https://doi.org/10.1144/jgs2017-107>.

Piercey, S.J. and Colpron, M. (2009): Composition and provenance of the Snowcap assemblage, basement to the Yukon-Tanana terrane, northern Cordillera: implications for Cordilleran crustal growth; Geosphere, v. 5, no. 5, p. 439–464, URL <https://doi.org/10.1130/GES00505.1>.

Rasbury, E.T. and Cole, J.M. (2009): Directly dating geologic events: U-Pb dating of carbonates; Reviews of Geophysics, v. 47, no. 3, URL <https://doi.org/10.1029/2007RG000246>.

Roberts, N.M.W., Drost, K, Horstwood, M.S.A., Condon, D.J., Chew, D., Drake, H., Milodowski, A.E., McLean, N.M., Smye, A.J., Walker, R.J., Haslam, H., Hodson, K., Imber, J., Beaudoin, N. and Lee, J.K. (2020): Laser ablation inductively coupled plasma mass spectrometry (LA-ICP-MS) U-Pb carbonate geochronology: strategies, progress, and limitations; Geochronology, v. 2, p. 33–61, URL <https://doi.org/10.5194/gchron-2-33-2020>.

Rodway, N. and Barrington, M. (2024): 2023 geological, geochemical, geophysical and diamond drilling report on the Blue property; BC Ministry of Energy, Mines and Low Carbon Innovation, Assessment Report 41885; 1142 p.

Seman, S., Stockli, D.F. and McLean, N.M. (2017): U-Pb geochronology of grossular-andradite garnet; Chemical Geology, v. 460, p. 106–116, URL <https://doi.org/10.1016/j.chemgeo.2017.04.020>.

Sillitoe, R.H. (2010): Porphyry copper systems; Economic Geology, v. 105, no. 1, p. 3–41, URL <https://doi.org/10.2113/gsecongeo.105.1.3>.

Soucy La Roche, R., Dyer, S.C., Zagorevski, A., Cottle, J.M. and Gaidies, F. (2022): 150 Myr of episodic metamorphism recorded in the Yukon-Tanana terrane, northern Canadian cordillera: evidence from monazite and xenotime petrochronology; Lithosphere, v. 2022, p. 7708357, URL <https://doi.org/10.2113/2022/7708357>.

Tizzard, A.M., Johnston, S.T. and Heaman, L.M. (2009): Arc imbrication during thick-skinned collision within the northern Cordilleran accretionary orogen, Yukon, Canada; Geological Society, London, Special Publications, v. 318, p. 309–327, URL <https://doi.org/10.1144/SP318.11>.

Yukon Geological Survey (2020): Yukon MINFILE – A database of mineral occurrences; Yukon Geological Survey, <https://data.geology.gov.yk.ca/Compilation/24> [May 2023].